

---

# Shortcut-connected Expert Parallelism for Accelerating Mixture-of-Experts

---

Weilin Cai Juyong Jiang Le Qin Junwei Cui Sunghun Kim Jiayi Huang\*  
The Hong Kong University of Science and Technology (Guangzhou)  
{wcai738, jjiang472, lqin674}@connect.hkust-gz.edu.cn  
{junweicui, hunkim, hjy}@hkust-gz.edu.cn

## Abstract

Expert parallelism has been introduced as a strategy to distribute the computational workload of sparsely-gated mixture-of-experts (MoE) models across multiple computing devices, facilitating the execution of these increasingly large-scale models. However, the *All-to-All communication* intrinsic to expert parallelism constitutes a significant overhead, diminishing the MoE models' efficiency. Current optimization approaches offer some relief, yet they are constrained by the sequential interdependence of communication and computation operations. To address this limitation, we present a novel shortcut-connected MoE architecture with overlapping parallel strategy, designated as ScMoE, which effectively decouples communication from its conventional sequence, allowing for a substantial overlap of **70%** to **100%** with computation. When compared with the prevalent top-2 MoE architecture, ScMoE demonstrates training speed improvements of **30%** and **11%**, and inference improvements of **40%** and **15%**, in our PCIe and NVLink hardware environments, respectively, where communication constitutes **60%** and **15%** of the total MoE time consumption. On the other hand, extensive experiments and theoretical analyses indicate that ScMoE not only achieves comparable but in some instances surpasses the model quality of existing approaches in vision and language tasks.

## 1 Introduction

In recent years, Transformer-based large language models (LLMs) have significantly propelled the fields of Natural Language Processing [54, 2, 57, 42, 56, 6, 1], Computer Vision [10, 31], and Multimodality [32, 68, 65, 70]. The sparsely-gated mixture-of-experts (MoE) approach has been integral in increasing parameter counts and enhancing model performance across various modalities [50, 48, 36, 25]. Expert parallelism [28, 13] has emerged as a viable strategy to distribute MoE computations efficiently over multiple devices, synergizing with conventional parallelism techniques [23, 52] such as data parallelism [45, 46] and model parallelism [38, 53].

Nevertheless, expert parallelism incurs substantial *All-to-All communication* overhead [28, 13], which can contribute to approximately 50% of the total time in intra-node multi-GPUs or multi-nodes distributed environments (see Figure 1), thus forming a critical bottleneck in scaling MoE models [40, 23, 33, 53]. Despite existing optimizations such as hierarchical All-to-All [20, 40] and pipelining [23, 66] strategies that mitigate communication delays and partially overlap communication with computation, the communication challenge persists due to the inherent sequential dependency between these operations [55]. To address this constraint, our intuitive idea is to reconstruct the inputs of MoE layer by incorporating not only the current-layer but also the preceding-layer representations through a shortcut connection, thereby refining the communication dependency and expanding the potential for optimization.

---

\*Corresponding author.

In this paper, we first introduce the DoubleGating MoE (DGMoE) architecture, which enables partial decoupling of inter-module communication, and further delineate the Shortcut MoE (ScMoE), which achieves complete decoupling of communication processes. Specifically, we build our architectures upon the standard top-2 MoE which typically substitutes the MLP module with a top-2 gating MoE module in every second transformer block (refer to the transformer block with MoE module as "current layer", and the preceding one without MoE module as "preceding layer"). Diverging from the top-2 process, our DGMoE employs dual top-1 gating mechanisms to independently manage the representations from the preceding and current layers, thereby decoupling the communication associated with the former one. Building on its MoE process of the preceding-layer representations, our ScMoE processes the current-layer representations using a dense MLP module and integrates the outcomes of both processing steps, thus eliminating the need for communication of current-layer representations.

To efficiently overlap the decoupled communication and computation within our shortcut-connected architectures, we implement an adaptive overlapping parallel strategy that dynamically schedules operators based on actual performance metrics. Relative to existing optimization strategies, our shortcut-connected approach not only doubles the overlap duration compared to the pipelining [22, 23] but also realizes complete overlapping of communication in scenarios where communication time does not surpass the computation duration. Furthermore, our method essentially advances the MoE architecture in algorithm aspect, which is device-agnostic to improve the efficiency of MoE model, thus ensuring a broad applicability across various hardware configurations and maintaining compatibility with current optimization techniques.

The extensive experimental results reveal that compared with the standard top-2 MoE, our ScMoE models achieve training speed improvements of 30% and 11% in  $8 \times A30$ -PCIe and  $8 \times A800$ -NVLink scenarios characterized by high and low communication overheads, respectively, and deliver inference speed improvements of 40% and 15%. Besides, our architecture has been demonstrated through experiments and theoretical analysis to attain or exceed the model quality of existing methods in both vision and language downstream tasks. In addition, through the analysis of experimental observations, we discuss the shortcut-connected MoE architectures and the differences between vision and language modalities from the MoE perspective. In summary, our contributions are:

- We propose shortcut-connected MoE architectures that break the conventional interdependency between communication and computation in distributed MoE models, bypassing the restrictions imposed on current communication optimization techniques.
- We develop an adaptive overlapping strategy for advancing expert parallelism with our shortcut-connected MoE, which significantly improves the efficiency of MoE models and ensures broad compatibility.
- We conduct empirical evaluation and theoretical analysis on our methods, confirming that our method accelerates MoE models while achieving comparable or even better model quality compared to existing methods.
- We explore the extension of shortcut-connected MoE and discuss the difference between vision and language modalities from the MoE standpoint, offering valuable perspectives for future research.

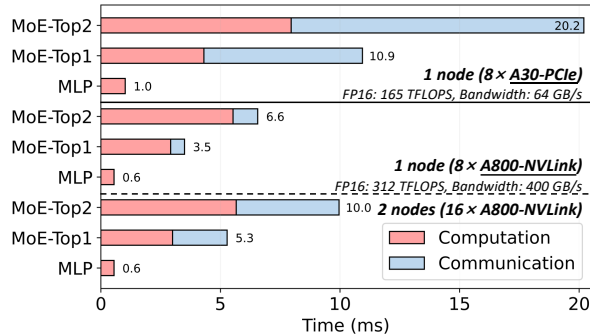


Figure 1: The overhead of MLP and top-2/top-1 MoE in a transformer block of SwinV2-MoE-S [23] model, allocating one expert per GPU with expert parallelism. The All-to-All communication takes up 60% of total time on a single node with  $8 \times A30$  GPUs, but drops to 15% on  $8 \times A800$  due to the latter’s  $6 \times$  higher bandwidth provided by GPU-to-GPU NVLink [14]. Despite benefiting from NVLink, communication still approaches 50% due to the lower-bandwidth inter-node Ethernet [30] when scaling across multiple nodes.

## 2 Background & Related Work

### 2.1 Sparsely-Gated Mixture-of-Experts

To expand the number of parameters in a neural network while taking into account the limitations of computational capacity, the work [50] presented a conditional computation method termed Sparsely-Gated Mixture-of-Experts (MoE). The MoE layer is composed of multiple feed-forward sub-networks, termed “experts”, and employs a trainable gating network to selectively activate a subset of these experts during each iteration. Given  $N$  expert networks  $\{E_i\}_1^N$ , gating network  $G$  and input representation  $x$ , the output of MoE module can be written:

$$MoE(x) = \sum_{i=1}^N G(x)_i E_i(x) \quad (1)$$

Following the prevailing approach in existing MoE research, we use the noisy top-k softmax gating network to select  $k$  experts for the computation, formalized by

$$G(x) = \text{Softmax}(\overline{\text{TopK}}(H(x), k)) \quad (2)$$

$$\overline{\text{TopK}}(H(x), k)_i = \begin{cases} H(x)_i, & \text{if } H(x)_i \in \text{TopK}(H(x)). \\ -\infty, & \text{otherwise.} \end{cases} \quad (3)$$

$$H(x)_i = (x \cdot W_{gate})_i + \epsilon_i, \quad (4)$$

$$\epsilon_i = \text{StandardNormal}() \cdot \text{Softplus}((x \cdot W_{noise})_i), \quad (5)$$

where  $\epsilon$  is tunable Gaussian noise,  $W_{gate}$  and  $W_{noise}$  denote two trainable weight matrices.

Leveraging sparse output of  $G(x)$ , this approach significantly increases the number of model parameters without causing a proportional increase in computational demand. The value of  $k$  can be set to 1 or 2 or even higher values. Opting for a larger  $k$  moves the model closer to the dense architecture, which generally results in higher prediction accuracy [48], but also leads to a substantial increase in execution overhead.

### 2.2 Expert Parallelism

To facilitate efficient distributed training and inference of MoE models, expert parallelism is proposed to allocate unique experts to each distributed computing device such as GPU and TPU, and map tokens to their corresponding experts through All-to-All communication across the participating devices [28, 19, 40]. As illustrated in Figure 2, the workflow of MoE employing expert parallelism is segmented into the following sequential operations: gate routing, input encode, All-to-All dispatch, expert computation, All-to-All combine, and output decode. To enhance the efficiency, input encode is employed to aggregate the token data layout to a contiguous format before All-to-All dispatch, and output decode is the inverse process after All-to-All combine. Furthermore, the integration of expert parallelism with other existing parallel strategies [23, 52, 13, 67] has been explored to support the scaling of larger MoE models on extensive distributed systems.

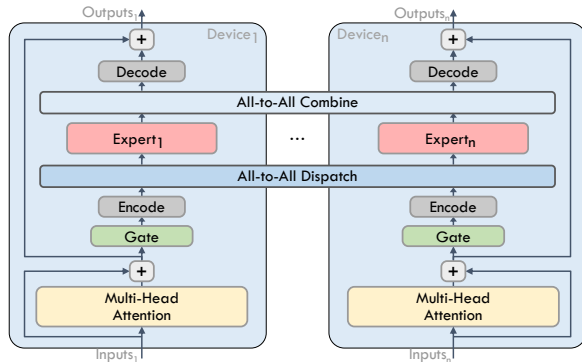


Figure 2: Illustration of scaling MoE transformer layer across multiple devices with expert parallelism.

### 2.3 Advancements for Mixture-of-Experts

As MoE models have exhibited noteworthy performance and potential, numerous studies are dedicated to enhancing the efficiency and accuracy of MoE models, as well as expanding MoE’s application

across diverse scenarios [51, 7, 18, 11, 62]. Due to the unique characteristics of Transformer-based MoE models, current algorithmic advancements for MoE primarily concentrate on refining gating strategies for expert selection and load balancing [29, 49, 47, 39], as these influence both efficiency and accuracy. Given the established efficacy of the original algorithm, some studies keep the same computation logic as the standard MoE proposed in GShard [28] and focus exclusively on enhancing the execution efficiency by optimizing operators [15, 69]. Besides, many studies endeavor to modify both the algorithm and system [20, 3, 64] in tandem to optimize execution efficiency without significantly losing model quality for MoE models, as this approach is widely favored and practical for large models [8, 5, 26]. For example, EdgeMoE [63] and Pre-gated MoE [24] incorporate information from preceding layers to predict the expert selection in current MoE layer, facilitating the preloading of expert parameters into the computational device’s memory in inference scenarios that cannot store the full MoE model. These approaches use preceding-layer representations only to decouple the expert selection (gate routing), with all other MoE operations following the original sequence and dependencies as delineated in Section 2.2, thus not enabling computation and communication overlap in distributed scenarios. In contrast, our shortcut-connected MoE treats the preceding-layer representations as inputs to current MoE layer, equal in status to the current-layer representations, allowing for the complete decoupling of all the MoE operations related to preceding-layer representations.

Specially, DeepSpeed-MoE [44] presented a novel MoE architecture called PR-MoE (combining Pyramid MoE and Residual MoE), which can be faster than standard top-2 MoE by reducing the communication volume while achieving on-par accuracy. In detail, Residual MoE fixes a dense MLP module to process all the input tokens and combines it with the result of top-1 gating expert for each token. In this paper, we introduce the MoE architectures analogous to DeepSpeed Residual MoE as the Fixed-MLP way, including (c) and (d) in Figure 3. In addition, the fixed-MLP architecture is not only rapidly increased in recent pre-trained MoE models such as OpenMoE [61] but also commonly employed in LoRA-based MoE model fine-tuning [58, 4, 18, 16].

### 3 Shortcut-connected MoE Architecture and Expert Parallelism

In the prevailing Transformer-based model, the MoE module substitutes MLP to sequentially manipulate intermediate representations [28, 12, 51], impeding the efficacy of existing communication optimization strategies [20, 40, 23, 66] due to the limited interaction within the MoE module.

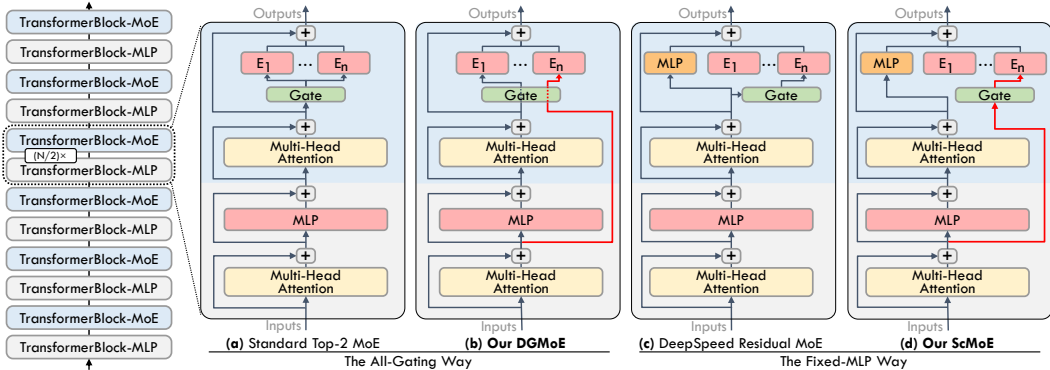


Figure 3: An overview of different MoE architectures. The red line represents the transmission of preceding-layer representations to the MoE via a shortcut connection. To streamline the explanation, details regarding pre-layer normalization (Pre-Norm) and dropout procedures have been excluded.

#### 3.1 Architectural Design

In this section, we propose two shortcut-connected MoE architectures, DGMoE and ScMoE, to eliminate the above limitations. Figure 3 provides a comprehensive depiction of the prevailing MoE architectures. We categorize these architectures into two categories given their gating mechanisms: (i) the All-Gating way, as employed in the standard MoE and our proposed DGMoE, and (ii) the

Fixed-MLP way, utilized in the DeepSpeed Residual MoE and our ScMoE. In particular, each MoE layer, denoted by a light blue block and referred to as TransformerBlock-MoE, replaces Multi-Layer Perceptron (MLP) in the Transformer architecture with a set of  $N$  specialized experts  $E_1, \dots, E_n$ . Following prior work[28, 12, 51, 23], the MoE layers are interspersed with a conventional Transformer layer, depicted as the gray block and termed TransformerBlock-MLP.

In our DGMoE architecture, delineated in Figure 3(b), we modify the standard top-2 gating mechanism (see Figure 3(a)) by employing dual top-1 gating mechanisms to independently manage the representations from the preceding and current layers, thereby decoupling the communication associated with the former one. Formally,

$$\mathcal{H}_{l+1}^{\text{DGMoE}} = \mathcal{H}_{l+1}^{\text{MH}} + \sum_{i=1}^N (G(\mathcal{H}_{l+1}^{\text{MH}})_i E_i(\mathcal{H}_{l+1}^{\text{MH}}) + G(\mathcal{H}_l^{\text{MH}})_i E_i(\mathcal{H}_l^{\text{MH}})) \quad (6)$$

$$\mathcal{H}_{l+1}^{\text{MH}} = \mathcal{H}_l^{\text{MLP}} + \text{MultiHead}_{\text{MoE}}^{(l+1)}(\mathcal{H}_l^{\text{MLP}}) \quad (7)$$

$$\mathcal{H}_l^{\text{MLP}} = \mathcal{H}_l^{\text{MH}} + \text{MLP}^{(l)}(\mathcal{H}_l^{\text{MH}}) \quad (8)$$

$$\mathcal{H}_l^{\text{MH}} = \mathcal{H}_{l-1} + \text{MultiHead}_{\text{MLP}}^{(l)}(\mathcal{H}_{l-1}) \quad (9)$$

where  $\mathcal{H}_{l+1}^{\text{DGMoE}}$  refers to the output from the MoE sub-layer,  $\mathcal{H}_{l+1}^{\text{MH}}$  signifies the output from the Multi-Head Attention (MultiHead) sub-layer  $\text{MultiHead}_{\text{MoE}}^{(l+1)}(\cdot)$  in the  $(l+1)$ -th TransformerBlock-MoE. The router  $G(\cdot)$  is referred to as Equation 2.  $\mathcal{H}_l^{\text{MLP}}$  and  $\mathcal{H}_l^{\text{MH}}$  are the outputs of the MLP sub-layer  $\text{MLP}^{(l)}(\cdot)$  and the MultiHead sub-layer  $\text{MultiHead}_{\text{MLP}}^{(l)}(\cdot)$ , respectively, in the  $l$ -th TransformerBlock-MLP. Note that we omit the pre-layer normalization (Pre-Norm) [59] and dropout operation for simplicity.

However, as delineated in Equation 6, a potential issue arises when a token at the current layer selects the same top-1 expert as the preceding layer, inadvertently collapsing the intended top-2 gating mechanism into a de facto top-1 gating mechanism. To mitigate this, we introduce a constraint that ensures the activation of two distinct experts. In practice, this is achieved by first documenting the indices of experts triggered by the preceding-layer representations. Subsequently, if the preceding-layer representation coincidentally targets the same expert as the current layer, that is, if  $\overline{\text{TopK}}(H(\mathcal{H}_l^{\text{MH}}), 1) = \overline{\text{TopK}}(H(\mathcal{H}_{l+1}^{\text{MH}}), 1)$ , we activate the second-highest-ranking expert from the top-2 selection for the current layer, *i.e.*,  $\overline{\text{TopK}}(H(\mathcal{H}_{l+1}^{\text{MH}}), 2)_2$ .

It is important to note that the DGMoE architecture facilitates only a partial decoupling of inter-module communication, due to the inherent communication bottlenecks presented by the current layer’s top-1 gating mechanism. In pursuit of fully decoupled communication pathways, we introduce the ScMoE depicted in Figure 3(d). The ScMoE architecture addresses the bottleneck by processing the current-layer representations through a dense MLP module. The outputs from this module are then combined with the outputs of top-1 gating-selected experts for the preceding-layer representations. Thus, our ScMoE effectively obviates the need for current-layer representation communication:

$$\mathcal{H}_{l+1}^{\text{ScMoE}} = \mathcal{H}_{l+1}^{\text{MH}} + \text{MLP}^{(l+1)}(\mathcal{H}_{l+1}^{\text{MH}}) + \sum_{i=1}^N G(\mathcal{H}_l^{\text{MH}})_i E_i(\mathcal{H}_l^{\text{MH}}) \quad (10)$$

where  $\mathcal{H}_{l+1}^{\text{ScMoE}}$  refers to the output from the MoE sub-layer in our ScMoE architecture, other notations remain consistent with those previously defined.

### 3.2 Theoretical Analysis

In this section, we delve deeper into the understanding of our proposed shortcut-connected MoE approaches, presenting a theoretical foundation focused on the propagation of gradients to guarantee consistent training and preserve model quality. Our analysis is confined to our ScMoE architecture as depicted in Figure 3(d); however, the same principles and derivations can be easily extended to our

DGMoE architecture. Building upon Equations 7 to 10, we can derive

$$\begin{aligned} \mathcal{H}_{l+1} = & \mathcal{H}_l^{MH} + \left( \text{MLP}^{(l)}(\mathcal{H}_l^{MH}) + \text{MultiHead}^{(l+1)}(\mathcal{H}_l^{MH} + \text{MLP}^{(l)}(\mathcal{H}_l^{MH})) \right) \\ & + \text{MLP}^{(l+1)}(\mathcal{H}_l^{MH} + \text{MLP}^{(l)}(\mathcal{H}_l^{MH})) + \text{MultiHead}^{(l+1)}(\mathcal{H}_l^{MH} + \text{MLP}^{(l)}(\mathcal{H}_l^{MH})) \\ & + \sum_{i=1}^N G(\mathcal{H}_l^{MH})_i E_i(\mathcal{H}_l^{MH}) \end{aligned} \quad (11)$$

$$\mathcal{H}_i^{MH} = \mathcal{H}_{l-1} + \text{MultiHead}^{(l)}(\mathcal{H}_{l-1}) \quad (12)$$

It is observable that Equations 11 and 12 share an identical structural expression. Consequently, we consider each pair of TransformerBlock-MoE and TransformerBlock-MLP layers as a single entity, and every sub-layer, denoted as  $\mathcal{F}$ , with its corresponding parameters  $\mathcal{W}_l$ , conforms to the equation

$$x_{l+1} = x_l + \mathcal{F}_{\mathcal{W}_l}(x_l) \quad (13)$$

Here,  $x_l$  represents the input, and  $x_{l+1}$  represents the output of the  $l$ -th sub-layer. By applying this relationship recursively, the output of the uppermost  $L$ -th sub-layer,  $x_L$ , can be deduced as follows

$$x_L = x_l + \sum_{i=l}^{L-1} \mathcal{F}_{\mathcal{W}_i}(x_l) \quad (14)$$

Let's consider the loss function as  $\mathcal{E}$ . Using the chain rule, we can calculate the derivative of the loss with respect to  $x_l$ , and we have

$$\frac{\partial \mathcal{E}}{\partial x_l} = \frac{\partial \mathcal{E}}{\partial x_L} \frac{\partial x_L}{\partial x_l} = \frac{\partial \mathcal{E}}{\partial x_L} \left( 1 + \frac{\partial}{\partial x_l} \sum_{i=1}^{L-1} \mathcal{F}_{\mathcal{W}_i}(x_i) \right) \quad (15)$$

It's clear that the additive component of the error gradient  $\frac{\partial \mathcal{E}}{\partial x_L}$  ensures direct information propagation back to any sub-layer  $x_l$ . Additionally, its advantage is that the number of product elements on the right side is independent of the network's depth. Therefore, as  $L$  increases, it is less likely to encounter the gradient vanishing or exploding problem, ensuring stable training and sustained performance levels in our proposed MoE architectures.

### 3.3 Overlapping Strategy for Expert Parallelism

As mentioned in the previous section, the MoE operations in ScMoE architecture are completely decoupled from the backbone network, enabling parallel execution across two independent streams: one for the Fixed-MLP process and another for the MoE process. To enhance the efficiency, we implement asynchronous All-to-All communication operators to enable the overlapping of communication and computation within these streams, while computation operators are unable to execute concurrently due to the constraints on computing resources. Moreover, we observe that operator execution times are influenced by the specific model and hardware configuration, necessitating the implementation of adaptive scheduling for operators.

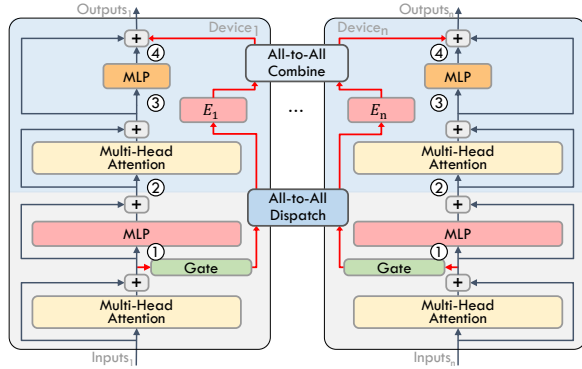


Figure 4: An overview of shortcut-connected expert parallelism for ScMoE. The red line represents the decoupled MoE stream and the numbers ① through ④ denote the potential locations for expert computation.

**Adaptive Operators Scheduling.** Following the execution order in the MoE stream, we can directly schedule the gate routing and encode operators at the earliest viable position while deferring the decode operator to the latest position, thereby maximizing the potential duration for overlapping. Then, this challenge is distilled into the selection of an optimal position for expert computation among four possible locations ①②③④ within the Fixed-MLP stream, as depicted in Figure 4. Formally,

we define the communication costs associated with ‘‘All-to-All Dispatch’’ and ‘‘All-to-All Combine’’ as  $\mathcal{T}_{disp}$  and  $\mathcal{T}_{comb}$ , respectively. The variable  $\mathcal{K}$  is designated to represent the specific location at which expert computation is applied. Prior to the expert computation, the computational costs are denoted as  $\mathcal{T}_{comp}^{pre} := \{COMP_1, \dots, COMP_{\mathcal{K}-1}\}$ , while the costs following the expert computation are represented as  $\mathcal{T}_{comp}^{post} := \{COMP_{\mathcal{K}+1}, \dots, COMP_4\}$ . Consequently, the minimal aggregate time cost for each pair consisting of one TransformerBlock-MLP and one TransformerBlock-MoE is

$$\begin{aligned} \mathcal{T}_{overall}^{block} &= \min_{\mathcal{K}} (|\mathcal{T}_{comp}^{pre} - \mathcal{T}_{disp}| + |\mathcal{T}_{comp}^{post} - \mathcal{T}_{comb}|) \\ &= \min_{\mathcal{K}} (|\sum_{i=1}^{\mathcal{K}-1} COMP_i - \mathcal{T}_{disp}| + |\sum_{i=\mathcal{K}+1}^4 COMP_i - \mathcal{T}_{comb}|) \end{aligned} \quad (16)$$

$$\mathcal{T}_{overall}^{block} \geq |(\mathcal{T}_{comp}^{pre} + \mathcal{T}_{comp}^{post}) - (\mathcal{T}_{disp} + \mathcal{T}_{comb})| \quad (17)$$

$$\mathcal{T}_{overall}^{block} \leq (\mathcal{T}_{comp}^{pre} + \mathcal{T}_{comp}^{post}) + (\mathcal{T}_{disp} + \mathcal{T}_{comb}) \quad (18)$$

To demonstrate the superior execution efficiency of our proposed overlapping parallel strategy, we have illustrated the operational timelines of various MoE architectures alongside their respective parallel strategies in Figure 5, exemplified by the selection of location ② for expert computation. Each timeline’s operator length corresponds to its execution time, and the presence of multiple rows signifies the utilization of parallel CUDA streams. The widely-used pipeline parallel strategy equally segments input tokens into smaller fine-grained data chunks, enabling concurrent computation and communication dispatched on distinct GPU streams [23, 66]. Contrary to standard MoE with pipelining (*2nd timeline*), our ScMoE with our proposed overlapping strategy (*4th timeline*) reduces the total communication time by half, leading to the same cost as the DeepSpeed Residual MoE (*3th timeline*). Our approach further optimizes performance by overlapping communication with a computation duration that includes two MLPs and one Multi-Head Attention, which extends beyond the duration of expert computation achieved through pipelining. Moreover, our strategy possesses the capability to fully overlap communication if the communication tasks can be accommodated within the overlapping window. This advantage is not shared by the pipeline strategy as it cannot overlap initial and terminal data transmissions [22, 37]. In cases where communication durations exceed the available overlap period, our strategy can be augmented with pipelining (*5th timeline*), thereby utilizing the expert computation duration to further hide communication. In addition, the proposed overlapping strategy is applicable to the decoupled part of MoE processing within DGMoE.

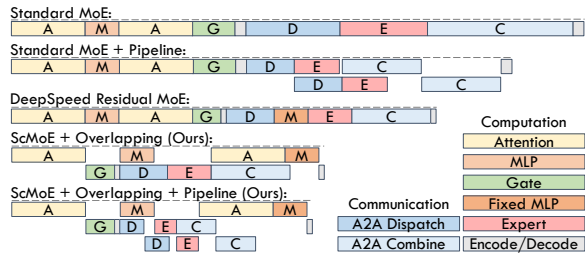


Figure 5: The timeline of different MoE architectures with corresponding parallel strategies, including pipeline and our proposed Overlapping. In each timeline, the length of each operator represents its time cost, while multiple rows indicate the utilization of parallel CUDA streams. The standard MoE uses top-2 gating.

## 4 Experiments

### 4.1 Experimental Setup

**Hardware Configurations.** We conduct experiments on two representative hardware configurations:  $8 \times A30$ -PCIe and  $8 \times A800$ -NVLink, exemplifying scenarios with high and low communication overheads, respectively, to evaluate the impact of the communication-to-computation ratio on the efficacy of our proposed overlapping strategy.

**Experiments on Vision Model.** To evaluate the efficacy of our MoE architectures on vision tasks, we conduct experiments on SwinV2-MoE model which is a state-of-the-art vision transformer model built upon the Tutel MoE framework [23, 31]. Specifically, we pre-train the SwinV2-MoE models with various MoE architectures on ImageNet-1K image classification dataset, and subsequently evaluate their accuracy on the corresponding test set. It is noteworthy that the integration of the MoE

module within SwinV2 is confined to stages 3 and 4, with our architectural enhancements being selectively applied to the MoE modules in stage 3 — the deepest submodel. Given our hardware constraints, we configure each MoE module with 8 experts, assigning one expert per GPU device.

**Experiments on Language Model.** For our natural language generation (NLG) tasks, we utilize the standard implementations of GPT-2 [43] and GPT-3 [2] from Fairseq [41], augmented with Tutel MoE to construct GPT2-MoE and GPT3-MoE models featuring an 8-expert MoE module. Specifically, we implement it by substituting the MLP with MoE in the second transformer block of every consecutive pair. Then, we pre-train the models with different architectures on OpenWebtext dataset [17]. In addition to assessing the pre-training validation perplexity, we also conduct a zero-shot evaluation of the pre-trained model on WikiText-103 [34] dataset.

Note that the experiments conducted on our shortcut-connected MoE models are accelerated through our overlapping parallel strategy. More setup details are illustrated in Appendix A.1.

Table 1: Test top-1 accuracy comparison and end-to-end speedup analysis of train/inference (iteration) for SwinV2-MoE-S [23] models with various architectures pre-trained on ImageNet-1K for 90 epochs in  $8 \times A30$ -PCIe scenario, using standard MoE with top-2 gating as the baseline.

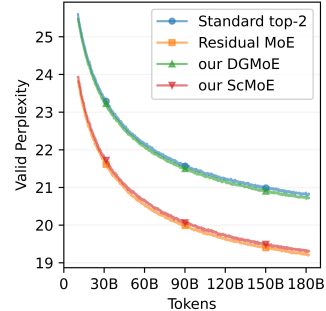
Model	ImageNet-1K (Acc@1 $\uparrow$ )	Train (Speedup $\uparrow$ )	Inference (Speedup $\uparrow$ )
Standard top-2	79.33%	1	1
Standard top-1	78.95%	1.27 $\times$	1.39 $\times$
Residual MoE	79.02%	1.24 $\times$	1.35 $\times$
Our DGMoE	<b>79.35%</b>	1.12 $\times$	1.18 $\times$
Our ScMoE	78.98%	<b>1.43<math>\times</math></b>	<b>1.66<math>\times</math></b>

Table 2: Comparison of zero-shot perplexity on WikiText-103 and end-to-end speedup analysis of train/inference (iteration) for our pre-trained GPT2-MoE-Medium [43] models with various architectures in  $8 \times A800$ -NVLink scenario, using standard MoE with top-2 gating as the baseline.

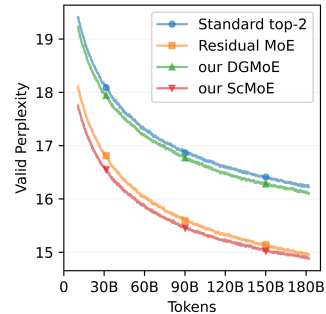
Model	WikiText-103 (Perplexity $\downarrow$ )	Train (Speedup $\uparrow$ )	Inference (Speedup $\uparrow$ )
Standard top-2	19.18	1	1
Residual MoE	17.94	1.04 $\times$	1.06 $\times$
Our DGMoE	18.97	1.01 $\times$	1.02 $\times$
Our ScMoE	<b>17.62</b>	<b>1.12<math>\times</math></b>	<b>1.17<math>\times</math></b>

## 4.2 Results and Analysis

**Vision Model.** We evaluate the model quality and execution efficiency of our experimental models with different MoE architectures on ImageNet-1K pre-training task. Table 1 illustrates that within the same MoE architecture category (see Figure 3), our DGMoE and standard top-2 MoE attain a comparable accuracy of 79.3%, while our ScMoE and Residual MoE achieve accuracy on par with standard top-1 at approximately 79.0%. However, in  $8 \times A30$ -PCIe scenario where communication overhead accounts for 60% of the total MoE time, our ScMoE model exhibits 30% speed improvement in training and 40% in inference compared to the standard top-2 MoE. Impressively, it even surpasses the top-1 MoE by 13% in training speed and 20% in inference. Besides, our DGMoE demonstrates a relatively modest speed improvement due to the incomplete decoupling and additional gating overhead. Consequently, our proposed shortcut-connected MoE architecture improves the MoE models’ operational efficiency without compromising on model quality. Additional experiments with the SwinV2-MoE-B model demonstrate similar results, as detailed in Appendix A.3.



(a) GPT2-MoE-Small



(b) GPT2-MoE-Medium

Figure 6: Token-wise validation perplexity curves for training MoE models with different MoE architectures.



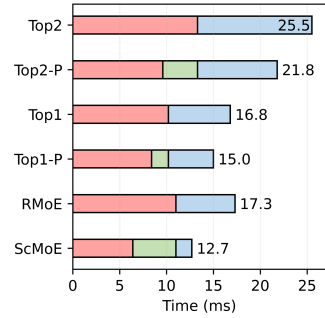
**Language Model.** As shown in Figure 6, the Fixed-MLP MoE architectures exhibit lower valid perplexity curves compared to the All-Gating MoE architectures during training in both the 12-layer GPT2-MoE-Small and 24-layer GPT2-MoE-Medium models. Consistently, in the zero-shot evaluation on the WikiText-103 dataset (see Table 2), the Fixed-MLP way yields lower perplexity, with our ScMoE achieving 17.62 and Residual MoE reaching 17.94, in contrast to the All-Gating way, which results in a perplexity of approximately 19. Different from the findings of the vision task, language models employing Fixed-MLP way notably outperform those with All-Gating way in terms of model quality, consistent with the findings in prior work [44]. As exemplified by the performance of two GPT2-MoE models, our methods perform high model quality across a range of network depths and potentially offer greater benefits in deeper networks, consistent with our theoretical analysis of shortcut connections. Additional zero-shot results of GPT2-MoE-Small are presented in Appendix A.3. Furthermore, our ScMoE achieves 11% speed improvement in training and 15% in inference compared to standard top-2 MoE in  $8\times A800$ -NVLink scenario, where communication constitutes 15% of the total MoE time. In contrast to our ScMoE, which is capable of significantly improving efficiency across various scenarios, our DGMoE achieves only a marginal acceleration in such a low communication overhead scenario.

**Analysis of Overhead and Acceleration.** In addition to exhibiting the significant end-to-end speedup of our ScMoE in Tables 1 and 2, we delve into a detailed analysis of the overhead and the acceleration effect with our overlapping strategy, which can be generalized to other Transformer-based MoE models. As illustrated in Figure 7, in the communication-intensive  $8\times A30$ -PCIe scenario, our ScMoE overlaps 70% communication time, resulting in 27% speed improvement compared to Residual MoE, even improving 15% compared to the pipelined standard top-1 MoE. In the  $8\times A800$ -NVLink setting, which features almost minimal communication overhead, our approach maintains acceleration, though the gains are comparatively modest. In general, our ScMoE delivers a significant acceleration over the standard top-2 MoE, and even outperforms the top-1 MoE when communication exceeds approximately 20% of the total MoE time. Besides, our ScMoE is capable of achieving complete communication overlapping in scenarios where communication does not exceed an estimated 50% of the total MoE time. It should be highlighted that our experiments were carried out within a single-node environment. Nevertheless, our experimental findings can be adapted to a broad spectrum of practical situations.

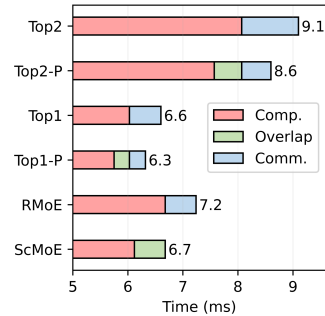
Figure 7: The overhead of each pair of TransformerBlock-MLP and TransformerBlock-MoE in SwinV2-MoE-S model in  $8\times A30$ -PCIe scenario (a) and  $8\times A800$ -NVLink scenario (b). “Topk” denotes the standard top-k MoE, while the one followed by the suffix “P” indicates using pipeline optimization as implemented by Tutel [23]. “RMoE” refers to DeepSpeed Residual MoE [44].

Table 3: Comparison of validation perplexity and end-to-end speedup analysis of train/inference (iteration) for our pre-trained GPT3-MoE-XL [2] models with various architectures in  $8\times A800$ -NVLink scenario, using standard MoE with top-2 gating as the baseline.

Model	Validation (Perplexity↓)	Train (Time Cost↓)	Inference (Time Cost↓)
Standard top-2	17.52	1.00×	1.00×
Our DGMoE	17.39	0.99×	0.98×
Our ScMoE	16.46	<b>0.89×</b>	<b>0.85×</b>
<hr/>			
Standard top-3	17.26	1.06×	1.09×
Our DGMoE-2	17.18	1.04×	1.06×
Our ScMoE-2	<b>16.27</b>	0.95×	0.93×



(a)  $8\times A30$ -PCIe



(b)  $8\times A800$ -NVLink

**Analysis of More Activated Experts.** As increasing the number of activated experts within standard MoE is correlated with enhancements in model quality, we implement this augmentation in our shortcut-connected MoE by increasing the count of experts which process the preceding-layer representations, while maintaining the process of current-layer representations. To investigate the benefits of more activated experts, we implement DGMoE-2 (top-2 experts for preceding-layer and top-1 expert for current-layer) and ScMoE-2 (top-2 experts for preceding-layer and one fixed MLP for current-layer). Comparative analyses with the standard top-3 MoE, which has same computational volumes as our DGMoE-2 and ScMoE-2, reveal that our shortcut-connected MoE architectures maintain superiority in both model quality and efficiency, as evidenced in Table 3. Furthermore, akin to the standard MoE, our MoE architectures demonstrate consistent performance enhancement with additional expert activation (e.g., a decrease in validation perplexity from 17.93 with DGMoE to 17.18 with DGMoE-2 and from 16.46 with ScMoE to 16.27 with ScMoE-2). Although activating more experts incurs higher time costs, the efficiency improvements of our overlapping strategy remain significant. For instance, our ScMoE-2 requires merely 95% and 93% of the time cost necessary for the standard top-2 MoE respectively in training and inference, despite processing increased computational loads.

**Analysis of Shortcut Representations.** To delve deeper into our shortcut connection, we conduct a series of experiments to compare the representations of the preceding layer and current layer for each MoE module, as illustrated in Figure 8. Specifically, after 10-epoch warm-up, we observe that: (a) lacking constraints on repeated expert selection, a trend wherein the token percentage of repeating expert selection initially escalates, peaking at 98%, and subsequently diminishes, with a significant drop manifested in the last MoE sub-layer. Hence, imposing restrictions on repeated expert selection is pivotal for attaining accuracy on par with the standard top-2 MoE; (b) analysis of the L2 distance (similarity) between preceding-layer and current-layer representations indicates that the L2 similarity initially decreases with network depth, then increases, and ultimately exhibits maximal value in the final layer; (c) the gating scores associated with representations from preceding layers grow quickly initially, converging thereafter, and achieving their maximum in the final MoE sub-layer; (d) the gating scores of current layer escalate from the first to the seventh MoE sub-layer, thereafter exhibiting a decline, yet growing sharply in the final layer. Additionally, the mean gating scores across all MoE sub-layers are around 0.2 ( $\pm 0.04$ ), noticeably lower than the 0.2 to 0.8 range for that of preceding layers. In summary, these insights highlight the importance of expert selection and their impact on model quality across varying network depths and training durations, calling for further investigations into the gating mechanism and its optimization.

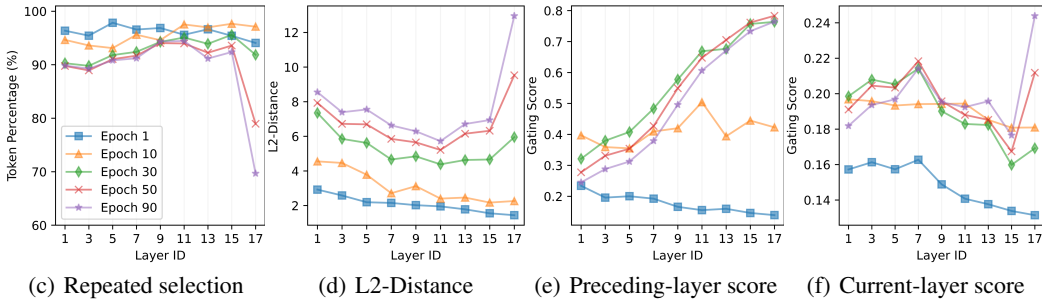


Figure 8: The comparison of preceding-layer and current-layer representations for MoE modules in SwinV2-MoE-S [23] model using DGMoE architecture in training progress. (a) denotes the percentage of tokens that retain the same expert selection across current layer and preceding layer. (b) denotes the L2 distance between these two representations. (c) denotes the average gating score of the preceding-layer representations. (d) denotes the average gating score of the current-layer representations.

**Analysis of MoE Discrepancy.** In our prior experimental analysis, we observe that the Fixed-MLP and All-Gating architectures demonstrate divergent model quality across vision and language tasks, suggesting a fundamental incongruity between the two modalities from the MoE perspective. As described in previous study [44], the Fixed-MLP approach employs a dense MLP module to learn from the entire training dataset, while treating the expert outputs from the MoE module as an

error correction mechanism to enhance the MLP’s predictions. Nonetheless, this method appears suboptimal for vision tasks, as it only attains an accuracy on par with the standard top-1 MoE. Considering the inherent disparities between word embeddings [35] and patch embeddings [10], we hypothesize that the merging of expert knowledge resembles a combinatorial operation for specific expert domains in vision, rather than a linear addition seemingly in language. For instance, the All-Gating way selects 2 experts out of 8 for a token, resulting in  $C_8^2 = 28$  unique combinations, while the Fixed-MLP way only yields  $1 \times C_8^1 = 8$  possible combinations, identical to the standard top-1 MoE. To further substantiate this hypothesis, we apply our ScMoE-2 on the vision task, which yields  $1 \times C_8^2 = 28$  possible combinations. Empirical results indicate that our ScMoE-2 attains an accuracy of 79.29%, commensurate with the 79.33% of the standard top-2 MoE.

## 5 Conclusion and Future Work

The inherent dependency of communication operations in distributed MoE models hinders parallel optimization techniques to improve execution efficiency. To overcome this, we propose a novel shortcut-connected MoE architecture called ScMoE, and develop a communication overlapping parallel strategy. Through comprehensive empirical evaluation and theoretical analysis, our approaches demonstrate better execution efficiency while maintaining, or exceeding, the model quality of existing methods in both vision and language tasks.

Additionally, we provide insightful analysis and discussion on the observations of shortcut-connected MoE architectures, as well as the MoE discrepancy between vision and language tasks, providing following perspectives for our future work: (1) From a certain point of view, our shortcut-connected MoE architectures can be conceptualized as the sharing of one MoE module across multiple transformer layers. Parameter sharing across different layers has been validated as a method to enhance parameter efficiency and improve model quality, as evidenced in existing research [27, 9, 60, 21]. As the preliminary experimental results presented in Appendix A.4, our shortcut-connected MoE architectures are potential to enhance model quality and efficiency by sharing MoE across more layers through shortcut connections. (2) The observations of MoE disparities between vision and language tasks prompt us to design multimodal MoE architectures, integrating modality-specific partial structures to optimize performance. (3) The optimization of training hyperparameters for the shortcut-connected MoE models requires more investigations.

## References

- [1] Josh Achiam, Steven Adler, Sandhini Agarwal, Lama Ahmad, Ilge Akkaya, Florencia Leoni Aleman, Diogo Almeida, Janko Altenschmidt, Sam Altman, Shyamal Anadkat, et al. Gpt-4 technical report. *arXiv preprint arXiv:2303.08774*, 2023.
- [2] Tom Brown, Benjamin Mann, Nick Ryder, Melanie Subbiah, Jared D Kaplan, Prafulla Dhariwal, Arvind Neelakantan, Pranav Shyam, Girish Sastry, Amanda Askell, et al. Language models are few-shot learners. *Advances in neural information processing systems*, 33:1877–1901, 2020.
- [3] Chang Chen, Min Li, Zhihua Wu, Dianhai Yu, and Chao Yang. Ta-moe: Topology-aware large scale mixture-of-expert training. *Advances in Neural Information Processing Systems*, 35:22173–22186, 2022.
- [4] Shaoxiang Chen, Zequn Jie, and Lin Ma. Llava-mole: Sparse mixture of lora experts for mitigating data conflicts in instruction finetuning mllms. *arXiv preprint arXiv:2401.16160*, 2024.
- [5] Krzysztof Marcin Choromanski, Valerii Likhoshesterov, David Dohan, Xingyou Song, Andreea Gane, Tamás Sarlós, Peter Hawkins, Jared Quincy Davis, Afroz Mohiuddin, Lukasz Kaiser, David Benjamin Belanger, Lucy J. Colwell, and Adrian Weller. Rethinking attention with performers. In *9th International Conference on Learning Representations, ICLR 2021, Virtual Event, Austria, May 3-7, 2021*. OpenReview.net, 2021.
- [6] Aakanksha Chowdhery, Sharan Narang, Jacob Devlin, Maarten Bosma, Gaurav Mishra, Adam Roberts, Paul Barham, Hyung Won Chung, Charles Sutton, Sebastian Gehrmann, et al. Palm: Scaling language modeling with pathways. *Journal of Machine Learning Research*, 24(240):1–113, 2023.

- [7] Damai Dai, Li Dong, Shuming Ma, Bo Zheng, Zhifang Sui, Baobao Chang, and Furu Wei. StableMoE: Stable routing strategy for mixture of experts. In Smaranda Muresan, Preslav Nakov, and Aline Villavicencio, editors, *Proceedings of the 60th Annual Meeting of the Association for Computational Linguistics (Volume 1: Long Papers)*, pages 7085–7095, Dublin, Ireland, May 2022. Association for Computational Linguistics.
- [8] Tri Dao, Dan Fu, Stefano Ermon, Atri Rudra, and Christopher Ré. Flashattention: Fast and memory-efficient exact attention with io-awareness. In S. Koyejo, S. Mohamed, A. Agarwal, D. Belgrave, K. Cho, and A. Oh, editors, *Advances in Neural Information Processing Systems*, volume 35, pages 16344–16359. Curran Associates, Inc., 2022.
- [9] Mostafa Dehghani, Stephan Gouws, Oriol Vinyals, Jakob Uszkoreit, and Lukasz Kaiser. Universal transformers. In *International Conference on Learning Representations*, 2018.
- [10] Alexey Dosovitskiy, Lucas Beyer, Alexander Kolesnikov, Dirk Weissenborn, Xiaohua Zhai, Thomas Unterthiner, Mostafa Dehghani, Matthias Minderer, Georg Heigold, Sylvain Gelly, Jakob Uszkoreit, and Neil Houlsby. An image is worth 16x16 words: Transformers for image recognition at scale. In *9th International Conference on Learning Representations, ICLR 2021, Virtual Event, Austria, May 3-7, 2021*. OpenReview.net, 2021.
- [11] Shihan Dou, Enyu Zhou, Yan Liu, Songyang Gao, Jun Zhao, Wei Shen, Yuhao Zhou, Zhiheng Xi, Xiao Wang, Xiaoran Fan, Shiliang Pu, Jiang Zhu, Rui Zheng, Tao Gui, Qi Zhang, and Xuanjing Huang. Loramoe: Revolutionizing mixture of experts for maintaining world knowledge in language model alignment. *CoRR*, abs/2312.09979, 2023.
- [12] Nan Du, Yanping Huang, Andrew M. Dai, Simon Tong, Dmitry Lepikhin, Yuanzhong Xu, Maxim Krikun, Yanqi Zhou, Adams Wei Yu, Orhan Firat, Barret Zoph, Liam Fedus, Maarten P. Bosma, Zongwei Zhou, Tao Wang, Yu Emma Wang, Kellie Webster, Marie Pellat, Kevin Robinson, Kathleen S. Meier-Hellstern, Toju Duke, Lucas Dixon, Kun Zhang, Quoc V. Le, Yonghui Wu, Zhifeng Chen, and Claire Cui. Glam: Efficient scaling of language models with mixture-of-experts. In Kamalika Chaudhuri, Stefanie Jegelka, Le Song, Csaba Szepesvári, Gang Niu, and Sivan Sabato, editors, *International Conference on Machine Learning, ICML 2022, 17-23 July 2022, Baltimore, Maryland, USA*, volume 162 of *Proceedings of Machine Learning Research*, pages 5547–5569. PMLR, 2022.
- [13] William Fedus, Barret Zoph, and Noam Shazeer. Switch transformers: Scaling to trillion parameter models with simple and efficient sparsity. *The Journal of Machine Learning Research*, 23(1):5232–5270, 2022.
- [14] Denis Foley and John Danskin. Ultra-performance pascal GPU and nvl link interconnect. *IEEE Micro*, 37(2):7–17, 2017.
- [15] Trevor Gale, Deepak Narayanan, Cliff Young, and Matei Zaharia. Megablocks: Efficient sparse training with mixture-of-experts. *CoRR*, abs/2211.15841, 2022.
- [16] Chongyang Gao, Kezhen Chen, Jinneng Rao, Baochen Sun, Ruibo Liu, Daiyi Peng, Yawen Zhang, Xiaoyuan Guo, Jie Yang, and VS Subrahmanian. Higher layers need more lora experts. *arXiv preprint arXiv:2402.08562*, 2024.
- [17] Aaron Gokaslan and Vanya Cohen. Openwebtext corpus. <http://Skylion007.github.io/OpenWebTextCorpus>, 2019.
- [18] Yunhao Gou, Zhili Liu, Kai Chen, Lanqing Hong, Hang Xu, Aoxue Li, Dit-Yan Yeung, James T. Kwok, and Yu Zhang. Mixture of cluster-conditional lora experts for vision-language instruction tuning. *CoRR*, abs/2312.12379, 2023.
- [19] Jiaao He, Jiezhong Qiu, Aohan Zeng, Zhilin Yang, Jidong Zhai, and Jie Tang. Fastmoe: A fast mixture-of-expert training system. *arXiv preprint arXiv:2103.13262*, 2021.
- [20] Jiaao He, Jidong Zhai, Tiago Antunes, Haojie Wang, Fuwen Luo, Shangfeng Shi, and Qin Li. Fastermoe: modeling and optimizing training of large-scale dynamic pre-trained models. In Jaejin Lee, Kunal Agrawal, and Michael F. Spear, editors, *PPoPP '22: 27th ACM SIGPLAN Symposium on Principles and Practice of Parallel Programming, Seoul, Republic of Korea, April 2 - 6, 2022*, pages 120–134. ACM, 2022.
- [21] Gao Huang, Zhuang Liu, Laurens van der Maaten, and Kilian Q. Weinberger. Densely connected convolutional networks. In *2017 IEEE Conference on Computer Vision and Pattern Recognition, CVPR 2017, Honolulu, HI, USA, July 21-26, 2017*, pages 2261–2269. IEEE Computer Society, 2017.

- [22] Yanping Huang, Youlong Cheng, Ankur Bapna, Orhan Firat, Dehao Chen, Mia Xu Chen, HyoukJoong Lee, Jiquan Ngiam, Quoc V. Le, Yonghui Wu, and Zhifeng Chen. Gpipe: Efficient training of giant neural networks using pipeline parallelism. In Hanna M. Wallach, Hugo Larochelle, Alina Beygelzimer, Florence d’Alché-Buc, Emily B. Fox, and Roman Garnett, editors, *Advances in Neural Information Processing Systems 32: Annual Conference on Neural Information Processing Systems 2019, NeurIPS 2019, December 8-14, 2019, Vancouver, BC, Canada*, pages 103–112, 2019.
- [23] Changho Hwang, Wei Cui, Yifan Xiong, Ziyue Yang, Ze Liu, Han Hu, Zilong Wang, Rafael Salas, Jithin Jose, Prabhat Ram, Joe Chau, Peng Cheng, Fan Yang, Mao Yang, and Yongqiang Xiong. Tutel: Adaptive mixture-of-experts at scale. *CoRR*, abs/2206.03382, 2022.
- [24] Ranggi Hwang, Jianyu Wei, Shijie Cao, Changho Hwang, Xiaohu Tang, Ting Cao, Mao Yang, and Minsoo Rhu. Pre-gated moe: An algorithm-system co-design for fast and scalable mixture-of-expert inference. *arXiv preprint arXiv:2308.12066*, 2023.
- [25] Albert Q Jiang, Alexandre Sablayrolles, Antoine Roux, Arthur Mensch, Blanche Savary, Chris Bamford, Devendra Singh Chaplot, Diego de las Casas, Emma Bou Hanna, Florian Bressand, et al. Mixtral of experts. *arXiv preprint arXiv:2401.04088*, 2024.
- [26] Nikita Kitaev, Lukasz Kaiser, and Anselm Levskaya. Reformer: The efficient transformer. In *8th International Conference on Learning Representations, ICLR 2020, Addis Ababa, Ethiopia, April 26-30, 2020*. OpenReview.net, 2020.
- [27] Zhenzhong Lan, Mingda Chen, Sebastian Goodman, Kevin Gimpel, Piyush Sharma, and Radu Soricut. Albert: A lite bert for self-supervised learning of language representations. In *International Conference on Learning Representations*, 2019.
- [28] Dmitry Lepikhin, HyoukJoong Lee, Yuanzhong Xu, Dehao Chen, Orhan Firat, Yanping Huang, Maxim Krikun, Noam Shazeer, and Zhifeng Chen. Gshard: Scaling giant models with conditional computation and automatic sharding. In *9th International Conference on Learning Representations, ICLR 2021, Virtual Event, Austria, May 3-7, 2021*. OpenReview.net, 2021.
- [29] Mike Lewis, Shruti Bhosale, Tim Dettmers, Naman Goyal, and Luke Zettlemoyer. BASE layers: Simplifying training of large, sparse models. In Marina Meila and Tong Zhang, editors, *Proceedings of the 38th International Conference on Machine Learning, ICML 2021, 18-24 July 2021, Virtual Event*, volume 139 of *Proceedings of Machine Learning Research*, pages 6265–6274. PMLR, 2021.
- [30] Ang Li, Shuaiwen Leon Song, Jieyang Chen, Jiajia Li, Xu Liu, Nathan R. Tallent, and Kevin J. Barker. Evaluating modern GPU interconnect: Pcie, nvlk, nvsl, nvswitch and gpudirect. *IEEE Trans. Parallel Distributed Syst.*, 31(1):94–110, 2020.
- [31] Ze Liu, Yutong Lin, Yue Cao, Han Hu, Yixuan Wei, Zheng Zhang, Stephen Lin, and Baining Guo. Swin transformer: Hierarchical vision transformer using shifted windows. In *2021 IEEE/CVF International Conference on Computer Vision, ICCV 2021, Montreal, QC, Canada, October 10-17, 2021*, pages 9992–10002. IEEE, 2021.
- [32] Jiasen Lu, Dhruv Batra, Devi Parikh, and Stefan Lee. Vilbert: Pretraining task-agnostic visiolinguistic representations for vision-and-language tasks. In Hanna M. Wallach, Hugo Larochelle, Alina Beygelzimer, Florence d’Alché-Buc, Emily B. Fox, and Roman Garnett, editors, *Advances in Neural Information Processing Systems 32: Annual Conference on Neural Information Processing Systems 2019, NeurIPS 2019, December 8-14, 2019, Vancouver, BC, Canada*, pages 13–23, 2019.
- [33] Ruben Mayer and Hans-Arno Jacobsen. Scalable deep learning on distributed infrastructures: Challenges, techniques, and tools. *ACM Computing Surveys (CSUR)*, 53(1):1–37, 2020.
- [34] Stephen Merity, Caiming Xiong, James Bradbury, and Richard Socher. Pointer sentinel mixture models. *arXiv preprint arXiv:1609.07843*, 2016.
- [35] Tomas Mikolov, Ilya Sutskever, Kai Chen, Greg S Corrado, and Jeff Dean. Distributed representations of words and phrases and their compositionality. In C.J. Burges, L. Bottou, M. Welling, Z. Ghahramani, and K.Q. Weinberger, editors, *Advances in Neural Information Processing Systems*, volume 26. Curran Associates, Inc., 2013.
- [36] Basil Mustafa, Carlos Riquelme, Joan Puigcerver, Rodolphe Jenatton, and Neil Houlsby. Multi-modal contrastive learning with limoe: the language-image mixture of experts. In Sanmi Koyejo,

- S. Mohamed, A. Agarwal, Danielle Belgrave, K. Cho, and A. Oh, editors, *Advances in Neural Information Processing Systems 35: Annual Conference on Neural Information Processing Systems 2022, NeurIPS 2022, New Orleans, LA, USA, November 28 - December 9, 2022*, 2022.
- [37] Deepak Narayanan, Aaron Harlap, Amar Phanishayee, Vivek Seshadri, Nikhil R. Devanur, Gregory R. Ganger, Phillip B. Gibbons, and Matei Zaharia. Pipedream: generalized pipeline parallelism for DNN training. In Tim Brecht and Carey Williamson, editors, *Proceedings of the 27th ACM Symposium on Operating Systems Principles, SOSP 2019, Huntsville, ON, Canada, October 27-30, 2019*, pages 1–15. ACM, 2019.
- [38] Deepak Narayanan, Mohammad Shoeybi, Jared Casper, Patrick LeGresley, Mostofa Patwary, Vijay Korthikanti, Dmitri Vainbrand, Prethvi Kashinkunti, Julie Bernauer, Bryan Catanzaro, Amar Phanishayee, and Matei Zaharia. Efficient large-scale language model training on GPU clusters using megatron-lm. In Bronis R. de Supinski, Mary W. Hall, and Todd Gamblin, editors, *International Conference for High Performance Computing, Networking, Storage and Analysis, SC 2021, St. Louis, Missouri, USA, November 14-19, 2021*, page 58. ACM, 2021.
- [39] Xiaonan Nie, Shijie Cao, Xupeng Miao, Lingxiao Ma, Jilong Xue, Youshan Miao, Zichao Yang, Zhi Yang, and Bin Cui. Dense-to-sparse gate for mixture-of-experts. *CoRR*, abs/2112.14397, 2021.
- [40] Xiaonan Nie, Pinxue Zhao, Xupeng Miao, Tong Zhao, and Bin Cui. Hetumoe: An efficient trillion-scale mixture-of-expert distributed training system. *CoRR*, abs/2203.14685, 2022.
- [41] Myle Ott, Sergey Edunov, Alexei Baevski, Angela Fan, Sam Gross, Nathan Ng, David Grangier, and Michael Auli. fairseq: A fast, extensible toolkit for sequence modeling. *arXiv preprint arXiv:1904.01038*, 2019.
- [42] Long Ouyang, Jeffrey Wu, Xu Jiang, Diogo Almeida, Carroll Wainwright, Pamela Mishkin, Chong Zhang, Sandhini Agarwal, Katarina Slama, Alex Ray, et al. Training language models to follow instructions with human feedback. *Advances in Neural Information Processing Systems*, 35:27730–27744, 2022.
- [43] Alec Radford, Jeffrey Wu, Rewon Child, David Luan, Dario Amodei, Ilya Sutskever, et al. Language models are unsupervised multitask learners. *OpenAI blog*, 1(8):9, 2019.
- [44] Samyam Rajbhandari, Conglong Li, Zhewei Yao, Minjia Zhang, Reza Yazdani Aminabadi, Ammar Ahmad Awan, Jeff Rasley, and Yuxiong He. Deepspeed-moe: Advancing mixture-of-experts inference and training to power next-generation ai scale. In *International Conference on Machine Learning*, pages 18332–18346. PMLR, 2022.
- [45] Samyam Rajbhandari, Jeff Rasley, Olatunji Ruwase, and Yuxiong He. Zero: Memory optimizations toward training trillion parameter models. In *SC20: International Conference for High Performance Computing, Networking, Storage and Analysis*, pages 1–16. IEEE, 2020.
- [46] Samyam Rajbhandari, Olatunji Ruwase, Jeff Rasley, Shaden Smith, and Yuxiong He. Zero-infinity: Breaking the gpu memory wall for extreme scale deep learning. In *Proceedings of the International Conference for High Performance Computing, Networking, Storage and Analysis*, pages 1–14, 2021.
- [47] Xiaozhe Ren, Pingyi Zhou, Xinfan Meng, Xinjing Huang, Yadao Wang, Weichao Wang, Pengfei Li, Xiaoda Zhang, Alexander Podolskiy, Grigory Arshinov, Andrey Bout, Irina Piontkovskaya, Jiansheng Wei, Xin Jiang, Teng Su, Qun Liu, and Jun Yao. Pangu- $\Sigma$ : Towards trillion parameter language model with sparse heterogeneous computing. *CoRR*, abs/2303.10845, 2023.
- [48] Carlos Riquelme, Joan Puigcerver, Basil Mustafa, Maxim Neumann, Rodolphe Jenatton, André Susano Pinto, Daniel Keysers, and Neil Houlsby. Scaling vision with sparse mixture of experts. In Marc’Aurelio Ranzato, Alina Beygelzimer, Yann N. Dauphin, Percy Liang, and Jennifer Wortman Vaughan, editors, *Advances in Neural Information Processing Systems 34: Annual Conference on Neural Information Processing Systems 2021, NeurIPS 2021, December 6-14, 2021, virtual*, pages 8583–8595, 2021.
- [49] Stephen Roller, Sainbayar Sukhbaatar, Arthur Szlam, and Jason Weston. Hash layers for large sparse models. In Marc’Aurelio Ranzato, Alina Beygelzimer, Yann N. Dauphin, Percy Liang, and Jennifer Wortman Vaughan, editors, *Advances in Neural Information Processing Systems 34: Annual Conference on Neural Information Processing Systems 2021, NeurIPS 2021, December 6-14, 2021, virtual*, pages 17555–17566, 2021.

- [50] Noam Shazeer, Azalia Mirhoseini, Krzysztof Maziarz, Andy Davis, Quoc V. Le, Geoffrey E. Hinton, and Jeff Dean. Outrageously large neural networks: The sparsely-gated mixture-of-experts layer. In *5th International Conference on Learning Representations, ICLR 2017, Toulon, France, April 24-26, 2017, Conference Track Proceedings*. OpenReview.net, 2017.
- [51] Sheng Shen, Zhewei Yao, Chunyuan Li, Trevor Darrell, Kurt Keutzer, and Yuxiong He. Scaling vision-language models with sparse mixture of experts. *arXiv preprint arXiv:2303.07226*, 2023.
- [52] Siddharth Singh, Olatunji Ruwase, Ammar Ahmad Awan, Samyam Rajbhandari, Yuxiong He, and Abhinav Bhatele. A hybrid tensor-expert-data parallelism approach to optimize mixture-of-experts training. In Kyle A. Gallivan, Efstratios Gallopoulos, Dimitrios S. Nikolopoulos, and Ramón Beivide, editors, *Proceedings of the 37th International Conference on Supercomputing, ICS 2023, Orlando, FL, USA, June 21-23, 2023*, pages 203–214. ACM, 2023.
- [53] Shaden Smith, Mostofa Patwary, Brandon Norrick, Patrick LeGresley, Samyam Rajbhandari, Jared Casper, Zhun Liu, Shrimai Prabhumoye, George Zerveas, Vijay Korthikanti, Elton Zheng, Rewon Child, Reza Yazdani Aminabadi, Julie Bernauer, Xia Song, Mohammad Shoeybi, Yuxiong He, Michael Houston, Saurabh Tiwary, and Bryan Catanzaro. Using deepspeed and megatron to train megatron-turing NLG 530b, A large-scale generative language model. *CoRR*, abs/2201.11990, 2022.
- [54] Ashish Vaswani, Noam Shazeer, Niki Parmar, Jakob Uszkoreit, Llion Jones, Aidan N. Gomez, Lukasz Kaiser, and Illia Polosukhin. Attention is all you need. In Isabelle Guyon, Ulrike von Luxburg, Samy Bengio, Hanna M. Wallach, Rob Fergus, S. V. N. Vishwanathan, and Roman Garnett, editors, *Advances in Neural Information Processing Systems 30: Annual Conference on Neural Information Processing Systems 2017, December 4-9, 2017, Long Beach, CA, USA*, pages 5998–6008, 2017.
- [55] Shibo Wang, Jinliang Wei, Amit Sabne, Andy Davis, Berkin Ilbeyi, Blake Hechtman, Dehao Chen, Karthik Srinivasa Murthy, Marcello Maggioni, Qiao Zhang, Sameer Kumar, Tongfei Guo, Yuanzhong Xu, and Zongwei Zhou. Overlap communication with dependent computation via decomposition in large deep learning models. In Tor M. Aamodt, Natalie D. Enright Jerger, and Michael M. Swift, editors, *Proceedings of the 28th ACM International Conference on Architectural Support for Programming Languages and Operating Systems, Volume 1, ASPLOS 2023, Vancouver, BC, Canada, March 25-29, 2023*, pages 93–106. ACM, 2023.
- [56] Jason Wei, Yi Tay, Rishi Bommasani, Colin Raffel, Barret Zoph, Sebastian Borgeaud, Dani Yogatama, Maarten Bosma, Denny Zhou, Donald Metzler, et al. Emergent abilities of large language models. *arXiv preprint arXiv:2206.07682*, 2022.
- [57] Jason Wei, Xuezhi Wang, Dale Schuurmans, Maarten Bosma, Fei Xia, Ed Chi, Quoc V Le, Denny Zhou, et al. Chain-of-thought prompting elicits reasoning in large language models. *Advances in Neural Information Processing Systems*, 35:24824–24837, 2022.
- [58] Xun Wu, Shaohan Huang, and Furu Wei. Mole: Mixture of lora experts. In *The Twelfth International Conference on Learning Representations*, 2023.
- [59] Ruibin Xiong, Yunchang Yang, Di He, Kai Zheng, Shuxin Zheng, Huishuai Zhang, Yanyan Lan, Liwei Wang, and Tie-Yan Liu. On layer normalization in the transformer architecture, 2020.
- [60] Fuzhao Xue, Ziji Shi, Futao Wei, Yuxuan Lou, Yong Liu, and Yang You. Go wider instead of deeper. In *Proceedings of the AAAI Conference on Artificial Intelligence*, volume 36, pages 8779–8787, 2022.
- [61] Fuzhao Xue, Zian Zheng, Yao Fu, Jinjie Ni, Zangwei Zheng, Wangchunshu Zhou, and Yang You. Openmoe: An early effort on open mixture-of-experts language models. *arXiv preprint arXiv:2402.01739*, 2024.
- [62] Rongjie Yi, Liwei Guo, Shiyun Wei, Ao Zhou, Shangguang Wang, and Mengwei Xu. Edgemoe: Fast on-device inference of moe-based large language models. *CoRR*, abs/2308.14352, 2023.
- [63] Rongjie Yi, Liwei Guo, Shiyun Wei, Ao Zhou, Shangguang Wang, and Mengwei Xu. Edgemoe: Fast on-device inference of moe-based large language models. *arXiv preprint arXiv:2308.14352*, 2023.
- [64] Mingshu Zhai, Jiaao He, Zixuan Ma, Zan Zong, Runqing Zhang, and Jidong Zhai. SmartMoE: Efficiently training Sparsely-Activated models through combining offline and online parallelization. In *2023 USENIX Annual Technical Conference (USENIX ATC 23)*, pages 961–975, Boston, MA, July 2023. USENIX Association.

- [65] Pengchuan Zhang, Xiujun Li, Xiaowei Hu, Jianwei Yang, Lei Zhang, Lijuan Wang, Yejin Choi, and Jianfeng Gao. Vinvl: Revisiting visual representations in vision-language models. In *Proceedings of the IEEE/CVF conference on computer vision and pattern recognition*, pages 5579–5588, 2021.
- [66] Zheng Zhang, Donglin Yang, Yaqi Xia, Liang Ding, Dacheng Tao, Xiaobo Zhou, and Dazhao Cheng. Mpipemoe: Memory efficient moe for pre-trained models with adaptive pipeline parallelism. In *IEEE International Parallel and Distributed Processing Symposium, IPDPS 2023, St. Petersburg, FL, USA, May 15-19, 2023*, pages 167–177. IEEE, 2023.
- [67] Lianmin Zheng, Zhuohan Li, Hao Zhang, Yonghao Zhuang, Zhifeng Chen, Yanping Huang, Yida Wang, Yuanzhong Xu, Danyang Zhuo, Eric P. Xing, Joseph E. Gonzalez, and Ion Stoica. Alpa: Automating inter- and intra-operator parallelism for distributed deep learning. In Marcos K. Aguilera and Hakim Weatherspoon, editors, *16th USENIX Symposium on Operating Systems Design and Implementation, OSDI 2022, Carlsbad, CA, USA, July 11-13, 2022*, pages 559–578. USENIX Association, 2022.
- [68] Kaiyang Zhou, Jingkang Yang, Chen Change Loy, and Ziwei Liu. Learning to prompt for vision-language models. *International Journal of Computer Vision*, 130(9):2337–2348, 2022.
- [69] Yanqi Zhou, Tao Lei, Hanxiao Liu, Nan Du, Yanping Huang, Vincent Zhao, Andrew M Dai, Quoc V Le, James Laudon, et al. Mixture-of-experts with expert choice routing. *Advances in Neural Information Processing Systems*, 35:7103–7114, 2022.
- [70] Deyao Zhu, Jun Chen, Xiaoqian Shen, Xiang Li, and Mohamed Elhoseiny. Minigpt-4: Enhancing vision-language understanding with advanced large language models. *arXiv preprint arXiv:2304.10592*, 2023.

## A Appendix

### A.1 Experimental Details

Table 4 summarizes the hyperparameters for training the Swin-MoE models including SwinV2-MoE-S and SwinV2-MoE-B. We develop our experiments based on the models and MoE framework which are provided by Tutel [23], and also follow its hyperparameter configurations. Then, we pre-train the models on ImageNet-1K image classification dataset. To maintain the comparability of our experiments, we limit our modifications solely to the MoE architectures and keep the hyperparameters consistent.

Table 4: Hyperparameters for SwinV2-MoE models.

Model	SwinV2-MoE-S	SwinV2-MoE-B
Image size	192×192	192×192
Window size	12×12	12×12
Embedding dim	96	128
Num. layers	[ 2, 2, 18, 2 ]	[ 2, 2, 18, 2 ]
Num. attention heads	[ 3, 6, 12, 24 ]	[ 4, 8, 16, 32 ]
Num. experts per layer	8	8
Num. parameters	157M	278M
Batch size	1024	1024
Epochs	90	90
Warmup epochs	10	10
Base LR	1.25e-4	1.25e-4
Warmup LR	1.25e-7	1.25e-7
Min LR	1.25e-6	1.25e-6
Capacity factor	1.25	1.25
MoE loss coefficient	0.01	0.01

Table 5 summarizes the hyperparameters for training the GPT-MoE models including GPT2-MoE-Small, GPT2-MoE-Medium and GPT3-MoE-XL. We implement our models based on the Fairseq [41] and Tutel [23] frameworks. And we use the Openwebtext dataset [17] for pre-training, with the GPT-2 BPE tokenizer [43]. In addition to evaluating the training curve, we also conduct a zero-shot



evaluation on WikiText-103 [34] dataset. Additionally, we maintained uniform hyperparameters across all models to ensure comparability, and we recognize that optimal parameter tuning may further enhance model performance, a subject for subsequent research.

Table 5: Hyperparameters for GPT2-MoE models.

Parameter	GPT2-MoE-Small	GPT2-MoE-Medium	GPT3-MoE-XL
Num. layers	12	24	24
Embedding dim	768	1024	2048
Num. attention heads	12	16	32
Num. experts per layer	8	8	8
Num. parameters	323M	1.1B	4.1B
Context/sequence length	1K	2K	2K
Training tokens	180B	180B	18B
Warmup tokens	100M	100M	10M
Batch size	256	64	32
Learning rate	1.0e-4	1.0e-4	1.0e-4
LR-Scheduler	Inverse_sqrt	Inverse_sqrt	Inverse_sqrt
Capacity factor	2.00	2.00	2.00
MoE loss coefficient	0.01	0.01	0.01

## A.2 Comprehensive Overview of Evaluated Architectures

As depicted in Figure 9, we provide a concise comparative overview of various MoE architectures, highlighting the differences between the standard top-1/top-2/top-3 MoE, DeepSpeed Residual MoE, our DGMoE, our ScMoE, our ScMoE-2, our DGMoE-2, and our DGMoE-Share.

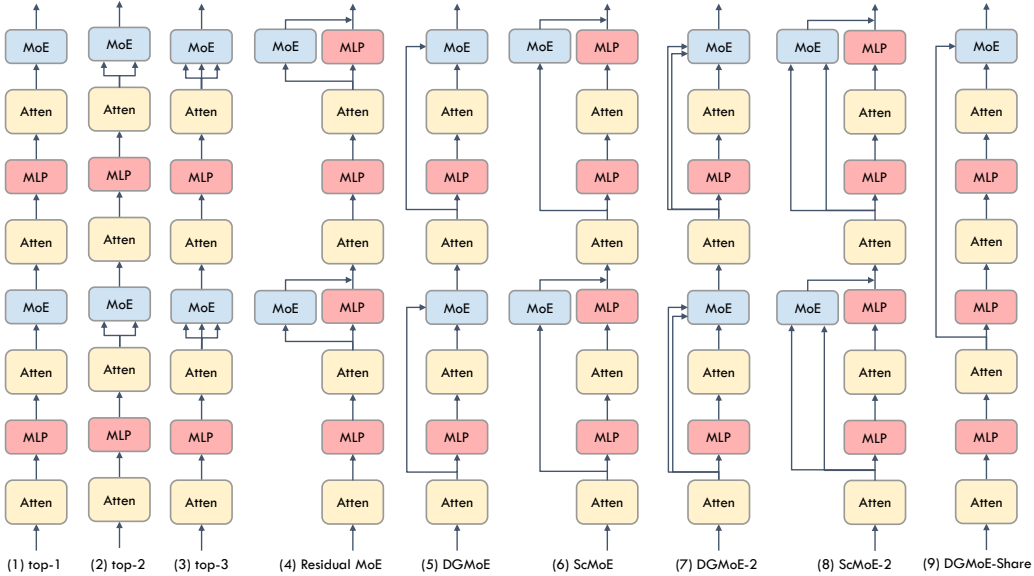


Figure 9: An overview of all the evaluated MoE architectures.

## A.3 Evaluation Across Different Model Sizes

Table 6 and Table 7 illustrate that within-category MoE architectures (Standard top-2 MoE and our DGMoE in the All-Gating way, DeepSpeed Residual MoE and our ScMoE in the Fixed-MLP way) consistently achieve analogous model quality across different model sizes, as expounded in the detailed analysis within the main body of this paper.

Table 6: Comparison of top-1 accuracy on the ImageNet-1K test set for SwinV2-MoE-S and SwinV2-MoE-B models with various architectures: top-2/top-1 gating standard MoE, Residual MoE, our DGMoE, and ScMoE, each pre-trained for 90 epochs on the ImageNet-1K classification dataset.

Model	SwinV2-MoE-S (Acc@1↑)	SwinV2-MoE-B (Acc@1↑)
Standard top-2	<b>79.33%</b>	<b>80.48%</b>
Standard top-1	78.95%	80.05%
Residual MoE	79.02%	80.10%
Our DGMoE	<b>79.35%</b>	<b>80.51%</b>
Our ScMoE	78.98%	80.07%

Table 7: Comparison of zero-shot perplexity on WikiText-103 for our pre-trained GPT-MoE-Small and GPT2-MoE-Medium models with various architectures.

Model	GPT2-MoE-Small (Perplexity↓)	GPT2-MoE-Medium (Perplexity↓)
Standard top-2	31.60	19.18
Residual MoE	<b>29.15</b>	<b>17.94</b>
Our DGMoE	31.52	18.91
Our ScMoE	<b>29.10</b>	<b>17.62</b>

#### A.4 Share MoE Across Multiple Layers via Shortcut Connections

The empirical analysis of our novel MoE architectures suggests that the MoE modules shared across multiple layers via shortcuts could offer a more parameter-efficient solution. We conduct experiments on a preliminary architecture DGMoE-Share (see Figure 9(9)) which shares a single MoE for two pairs of transformer blocks. It reduces the parameter count from 157M to 124M, while maintaining the same volume of expert computation as the standard top-1 MoE. The DGMoE-Share achieves a 78.45% accuracy on the vision task, incurring a minimal accuracy decrement of 0.5% relative to the standard top-1 MoE. We anticipate the discovery of more efficient architectures through future explorations.

#### A.5 Weighted Addition for Fixed-MLP

In prior research, DeepSpeed Residual MoE [44] employs a straightforward additive approach to integrate the outputs from the fixed MLP and the MoE module, whereas MoCLE [18] implements a weighted addition mechanism that adjusts the fixed MLP output by a factor of  $(1 - G_{max})$ , with  $G_{max}$  representing the top-1 gating score within the MoE. Recognizing the diverse array of shortcut connections employed across various fields, we also consider exploring the impact of various integration methods for combining the outputs from the fixed MLP and the MoE. Therefore, we investigate the efficacy of implementing a simple constant weighted addition method for our ScMoE. For example, we can set a weight of 0.2, approximating the gating score for current-layer representations in our DGMoE. The experiments with varying weights reveal a subtle influence on model quality, yielding an accuracy of approximately  $78.90\% \pm 0.2\%$ . This effect is relatively insignificant compared to the enhancements achieved through architectural modifications or alterations to the top-k gating parameter.